РОССИЙСКАЯ АКАДЕМИЯ НАУК

ПИСЬМА
В ЖУРНАЛ ЭКСПЕРИМЕНТАЛЬНОЙ
И ТЕОРЕТИЧЕСКОЙ ФИЗИКИ

ОСНОВАН В 1965 ГОДУ *ТОМ 68, ВЫПУСК 3*
ВЫХОДИТ 24 РАЗА В ГОД *10 АВГУСТА, 1998*

Pis'ma v ZhETF, vol.68, iss.3, pp.161 - 166

TOWARDS A UNIVERSAL NUCLEAR DENSITY FUNCTIONAL

S.A.Fayans

Russian Research Centre - "Kurchatov Institute"
123182 Moscow, Russia

Submitted 16 June 1998

A new form of the nuclear energy-density functional for describing the ground state properties of finite nuclei up to the drip lines and beyond is proposed. The volume part in this functional fits the Friedman – Pandharipande and Wiringa – Fiks – Fabrocini equation of sate, for the UV14 plus TNI model up to the densities $\rho \approx 1$ fm^{-3}, by a fractional expression in ρ which can be extended to higher densities preserving causality. For inhomogeneous systems, a surface energy-density term is added, with two free parameters, which also has a fractional form like the Padé approximant containing $(\nabla\rho)^2$ both in the numerator and in the denominator. In addition to the Coulomb direct and exchange interaction energy, an effective ρ-dependent Coulomb-nuclear correlation term is included with one more free parameter. A three-parameter fit to the masses and radii of real nuclei shows that the latter term gives contribution of the same order of magnitude as the Nolen – Schiffer anomaly in Coulomb displacement energy. The first self-consistent run with the suggested functional, performed for about 100 spherical nuclei, has given the rms deviations from the experiment of ≈ 1.2 MeV in masses and ≈ 0.01 fm in radii, which is about a factor of two better than those obtained with the Skyrme functionals or with the Gogny force. The extrapolation to the drip lines goes in between the ETFSI and the macroscopic-microscopic model predictions.

PACS: 21.10.Dr, 21.65.+f

Recent progress in measuring the basic nuclear properties such as nuclear mases and radii as well as the increase in accumulating nuclear data is very impressive. Physics with radioactive beams has opened new era in experimental studies of nuclei not too far from the beta stability valley and of nuclear exotica at extreme N/Z ratios up to the drip lines and beyond. From theoretical side, unfortunately, the present-day microscopic approaches are not able either to describe the properties of already known nuclei with sufficient accuracy to meet modern experiments or to give reliable predictions for nuclear terra incognita and, specifically, for the data needed for the astrophysical applications which are not expected to be measured in the nearest future. Among existing approaches, the most successful are the self-consistent mean-field microscopic models based on the effective

energy-density functionals (EDF) incorporating forces of Skyrme type with zero range or of Gogny type with finite range, and also the relativistic mean field (RMF) model with classical meson fields. These models can give the masses and radii of measured nuclei with the respective rms deviations of no better than about 2 MeV and 0.02 fm from experiment [1]. They may differ in the extrapolation behavior [2] but, most importantly, all their predictions, already for nuclei not too far from stability, are in striking deviation from those of the macroscopic-microscopic (MM) models [3] or of the extended Tomas – Fermi model with Strutinsky integral (ETFSI) [4]. These latter models are able to reproduce the measured nuclear masses and charge radii with the rms error down to ≈ 0.6 MeV and ≈ 0.02 fm, respectively, and their predictions are currently considered to be the most reliable. Such a large disagreement between the two approaches may indicate that some important physical ingredients are missing in the EDF construction, and perhaps the form of the EDF used so far in the microscopic calculations is not flexible enough to effectively incorporate them. Searches for a better parameter set for these "old" functionals are still continuing (see, e.g., a very recent paper [5] where the Skyrme functionals are revisited with respect to the isovector $\propto (N-Z)^2$ component but it is hard to believe that this revision would cure the above disagreement).

In suggesting a new EDF, two issues should be kept in mind. Firstly, in changing the conventional EDF form, in an attempt to improve the description of nuclear masses and radii, it is highly desirable to reach a mutually consistent result: the relative error for both these quantities should be of the same order. As one may notice, this is not the case with all available calculations since they yield relative rms deviations for radii that are a factor of 4 worse than those for binding energies. Secondly, it would be of great advantange if a new EDF could be used not only for nuclei throughout the nuclear chart but also for describing such objects as neutron stars, with the crystal structure in their crust. The present paper is an attempt towards such a universal nuclear density functional.

The total energy density of a nuclear system is represented as

$$\varepsilon = \varepsilon_{kin} + \varepsilon_v + \varepsilon_s + \varepsilon_{Coul} + \varepsilon_{sl} + \varepsilon_{anomal} \ , \tag{1}$$

where ε_{kin} is the kinetic energy term which, since we are constructing a Kohn-Sham type functional, is taken with the free operator $t = p^2/2m$, i.e. with the effective mass $m^* = m$; all the other terms are discussed below.

The volume term in (1) is chosen to be in the form

$$\varepsilon_v = \frac{2}{3}\epsilon_F^0 \rho_0 \left[a_+^v \frac{1 - h_{1+}^v x_+^\sigma}{1 + h_{2+}^v x_+^\sigma} x_+^2 + a_-^v \frac{1 - h_{1-}^v x_+}{1 + h_{2-}^v x_+} x_-^2 \right] . \tag{2}$$

Here and in the following $x_\pm = (\rho_n \pm \rho_p)/2\rho_0$, $\rho_{n(p)}$ is the neutron(proton) density, $2\rho_0$ is the equilibrium density of symmetric nuclear matter with $\varepsilon_F^0 = (9\pi/8)^{2/3}\hbar^2/2mr_0^2$, the Fermi energy and $r_0 = (3\pi\rho_0/8)^{1/3}$, the radius parameter. The fractional expressions of the type of eq. (2) were introduced in [6] for the EDF with application to finite systems with pairing correlations. Such expressions allow an extrapolation of nuclear equation of state (EOS) to very high densities while preserving causal behavior. This might be of advantage since the available microscopic nuclear matter EOS often violate causality at $\rho > 1$ fm^{-3}. Thus, in deriving the parameters of eq. (2), we shall use the EOS of refs. [7, 8] only in the region of up to about six times the saturation density.

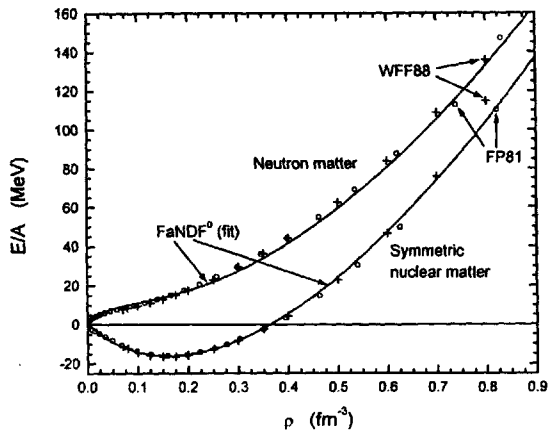

Fig.1. Binding energy per nucleon in symmetric nuclear matter and in neutron matter. Open circles and crosses are the calculations of ref. [7] and ref. [8], respectively. The solid lines show the fit by fractional expressions of eq. (2)

The four parameters in the isoscalar volume energy density $\propto a_+^v$ are fixed by fitting to the EOS of symmetric infinite nuclear matter [7, 8] for the UV14 plus TNI model. The result shown in fig. 1 by the lower solid curve is obtained with the exponent $\sigma = 1/3$, the compression modulus $K_0 = 220$ MeV, the equilibrium density $2\rho_0 = 0.16$ fm^{-3} ($r_0 = 1.143$ fm) and the chemical potential $\mu = -16.0$ MeV (the energy per nucleon at saturation point). The dimensionless parametres are $a_+^v = -9.559$, $h_{1+}^v = 0.633$, $h_{2+}^v = 0.131$. Keeping them fixed, a fit to the neutron matter EOS from the same papers [7, 8] is performed to determine the three parameters of the isovector part $\propto a_-^v$ in eq.(1). Good description presented in fig. 1 by the upper solid curve is obtained with $a_-^v = 4.428$, $h_{1-}^v = 0.250$, $h_{2-}^v = 1.300$. This corresponds to the asymmetry energy coefficient $\beta_0 = 30.0$ MeV. Note that, according to our fit, the asymmetry energy decreases with ρ, changing sign at four times saturation density. Such a behavior might lead to the neutron-proton separation instability in dense matter [9].

The surface part in eq. (1) is meant to describe the finite-range and nonlocal in-medium effects which, phenomenologically, may presumably be incorporated within the EDF framework in a localized form by introducing a dependence on density gradients. It is taken as follows:

$$\varepsilon_s = \frac{2}{3}\epsilon_F^0\rho_0 \frac{a_+^s r_0^2(\nabla x_+)^2}{1 + h_+^s x_+^\sigma + h_\nabla^s r_0^2(\nabla x_+)^2}\,, \tag{3}$$

with $h_+^s = h_{2+}^v$, a_+^s and h_∇^s the two free parameters. Such a form is obtained by adding the terms $\propto (\nabla x_+)^2$ *both* in the numerator *and* in the denominator of the isoscalar volume energy density of eq. (2). Alternatively, this peculiar surface term may be regarded as the Padé approximant for the (unknown) expansion in $(\nabla\rho)^2/(1 + h_+^s x_+^\sigma)$ where the form factor $1/(1 + h_+^s x_+^\sigma)$ imitates a transformation to the Migdal's quasiparticles (cf. ref. [10]). In fact, h_+^s is also a free parameter but here we prefer to keep it fixed by the above condition.

The Coulomb part in eq. (1) is approximated by

$$\varepsilon_{Coul} = 2\pi e^2 \rho_{ch}(r)\left(\frac{1}{r}\int_0^r \rho_{ch}(r)r^2\,dr + \int_r^\infty \rho_{ch}(r)r\,dr\right) - \frac{3}{4}\left(\frac{3}{\pi}\right)^{1/3} e^2 \rho_p^{4/3}(1 - h_{Coul}x_+^\sigma)\,, \tag{4}$$

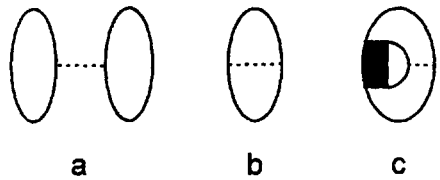

Fig.2. Representative diagrams that can contribute to the Coulomb-induced binding energy. Diagrams *a* and *b* correspond to direct and exchange Coulomb term, respectively, whereas diagram *c* shows Coulomb-nuclear correlation term. The solid lines represent the nucleon (proton) Green's function, dashed lines the Coulomb interaction, the black square the total amplitude of NN (proton-proton) interaction

where the first term, diagram fig. 2a, is the direct Coulomb contribution (expressed through charge density ρ_{ch} and written, for simplicity, for the case of the spherical symmetry), while the second term is the exchange part, fig. 2b, taken in the Slater approximation and combined with the Coulomb-nuclear correlation term $\propto h_{Coul}$, fig. 2c. The latter is believed to account for the correlated motion of protons in nuclei beyond the direct (Hartree) and exchange (Fock) Coulomb interaction [11, 12].

The spin–orbit term ε_{sl} in eq. (1) comes from the two-body spin-orbit interaction $\propto (\kappa + \kappa' \tau_1 \cdot \tau_2)[\nabla_1 \delta(\mathbf{r}_1 - \mathbf{r}_2) \times (\mathbf{p}_1 - \mathbf{p}_2)] \cdot (\sigma_1 + \sigma_2)$. For spherical nuclei one gets

$$\varepsilon_{sl} = C_0 r_0^2 \sum_{i,k=n,p} \frac{1}{r} \rho_{sl}^i \kappa^{ik} \frac{d\rho^k}{dr}\,, \tag{5}$$

where ρ_{sl} is the spin–orbit density, $\rho_{sl}^{n,p}(\mathbf{r}) = \sum_\lambda n_\lambda \langle \sigma \cdot \mathbf{l} \rangle_\lambda \mid \varphi_\lambda^{n,p}(\mathbf{r}) \mid^2$ with n_λ the occupation number of the single-particle level λ, φ_λ its wave function, $\langle \sigma \cdot \mathbf{l} \rangle_\lambda = j(j+1) - l(l+1) - 3/4$, $\kappa^{nn} = \kappa^{pp} = \kappa + \kappa'$, $\kappa^{np} = \kappa^{pn} = \kappa - \kappa'$, and $C_0 = 2\varepsilon_F^0/3\rho_0$ the inverse density of states on the Fermi surface ($C_0 = 307.2$ MeV·fm^{-3}). It is known from the RMF theory that the isovector spin-orbit force is very small compared to the isoscalar one [13]. Thus we set $\kappa' = 0$ and derive the isoscalar strength $\kappa = 0.19$ from the average description of the splitting of the single-particle states in ^{208}Pb.

The last term in eq. (1), the anomalous energy density, is represented as

$$\varepsilon_{anomal} = \sum_{i=n,p} C_0 \nu^{\dagger i}(\mathbf{r}) f^\xi(x_+(\mathbf{r})) \nu^i(\mathbf{r})\,, \tag{6}$$

where $\nu(\mathbf{r})$ is the anomalous density and $C_0 f^\xi$ is the effective force in the particle–particle channel with the dimensionless formfactor [12] $f^\xi(x_+) = f_{ex}^\xi + h^\xi x_+ + f_\nabla^\xi r_0^2 (\nabla x_+)^2$. The strength parameters $f_{ex}^\xi = -2.8$, $h^\xi = 2.8$ and $f_\nabla^\xi = 2.2$ are extracted from a fit to the neutron separation energies and charge radii of lead isotopes [12].

The three parameters a_+^s, h_∇^s and h_{Coul} remain to be defined. This was done through a χ^2 fit to the masses and radii of about 100 spherical nuclei from ^{38}Ca to ^{220}Th with the result $a_+^s = 0.600$, $h_\nabla^s = 0.440$ and $h_{Coul} = 0.941$, the rms deviations being 1.2 MeV and 0.01 fm for masses and radii, respectively. We shall call the EDF in the suggested form, with the just extracted parameters, the Nuclear Density Functional FaNDF^0 (superscript 0 means a "zero" approximation in the sense that other parameter sets, FaNDF^i, $i = 2$, 3,..., might be found leading to a better fit).

Typical results of the spherical HF+BCS calculations with FaNDF^0 are shown in fig. 3 for even Pb isotopes, from the proton drip line to the neutron drip line (47 nuclides), in comparison with experimental data and other model predictions. The ETFSI model is chosen as a reference. The nuclei in the $A \approx 222$ to 248 region might have a static

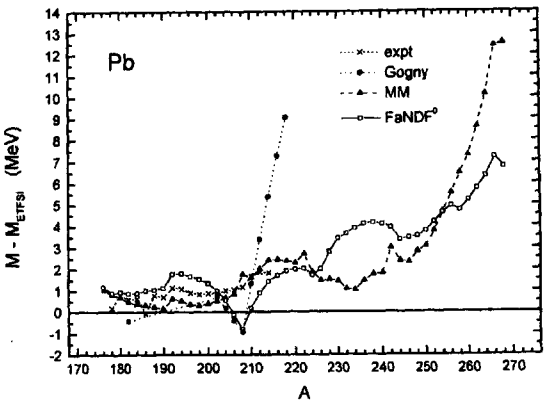

Fig.3. Deviations of various theoretical masses from the ETFSI mass [4] for a long chain of lead isotopes. Black triangles correspond to the MM model [3], solid dots to the Gogny force (from [2]). The results obtained with FaNDF^0 are shown by open squares. The experimentally known masses including those derived from systematics [15] are presented by crosses

deformation [3, 4], so one expects that, with deformed code, the results for FaNDF^0 in this region will be shifted down closer to the MM or ETFSI results. Analogous calculations for tin isotopes are presented in fig. 4. It is seen that the predictions obtained with the Gogny force just outside the measured regions are in strong disagreement with other models. Approaching the neutron drip line, the masses obtained with FaNDF^0 fall in between the MM and ETFSI predictions.

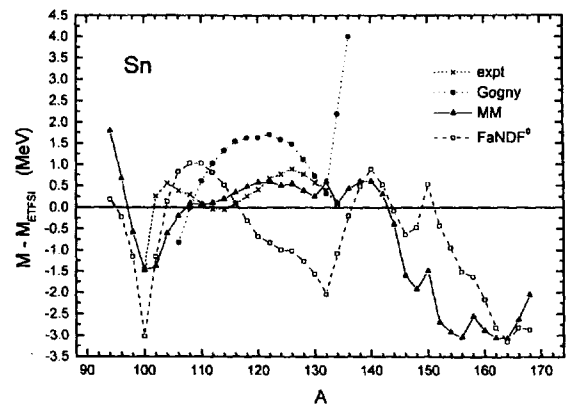

Fig.4. The same as in fig. 3 but for the chain of tin isotopes

Finally, the mass differences for the mirror nuclei ^{17}F-^{17}O and ^{41}Sc-^{41}Ca calculated with FaNDF^0 in the uniform filling approximation are 3.546 MeV and 7.174 MeV, respectively, whereas the corresponding experimental values are 3.543 MeV and 7.278 MeV. In all calculations the nucleon charge form factors in the direct Coulomb term and neutron-proton mass difference in the free kinetic energy operator are always taken into account. Omitting the Coulomb-nuclear correlation term by setting $h_{Coul} = 0$, the calculated mass differences for these mirror pairs would be respectively 3.300 MeV and 6.872 MeV leading to a 6-7% discrepancy; this kind of discrepancy is known as the Nolen-Schiffer anomaly. It follows that Coulomb-nuclear correlations play an important role in finite nuclei. Incorporating the corresponding term in the EDF improves the description of nuclear ground state properties and greatly reduces the severity of the Nolen-Schiffer anomaly.

To summarize, we have shown that the agreement between microscopic self-consistent theory and experiment is significantly improved with the proposed EDF in which the volume part fits the microscopic EOS for infinite uniform matter, the surface term has a peculiar form as given by eq. (3) and, for finite systems, the Coulomb part contains an additional Coulomb-nuclear correlation term. The first resuts obtained with the FaNDF^0 parametrization are encouraging. The proposed construction of the EDF seems to be an important step towards a universal nuclear density functional.

The author thanks J.Wambach for usefull discussions concerning the microscopic nuclear matter EOS during the early stage of this work, and expresses his gratitude to V.Shaginyan, S.Tolokonnikov and D.Zawischa for their continuous interest and helpful comments. This work was supported by the Russian Foundation for Basic Research through the Grant 98-02-16979. The computations have been performed on a computer provided by the Deutsche Forschungsgemeinschaft.

---

1. Pomorski, P.Ring, G.A.Lalazissis et al., Nucl. Phys. **A624**, 349 (1997).
2. Z.Patyk, A.Baran, J.F.Berger et al., GSI-Preprint-97-40, August 1997.
3. P.Möller, J.R.Nix, W.D.Myers, and W.J.Swiatecki, At. Data Nucl. Data Tables **59**, 185 (1995).
4. Y.Aboussir, J.M.Pearson, A.K.Dutta, and F.Tondeur, At. Data Nucl. Data Tables **61**, 127 (1995).
5. E.Chabanat, P.Bonche, P.Haensel et al., Nucl. Phys. **A627**, 710 (1997).
6. A.V.Smirnov, S.V.Tolokonnikov, and S.A.Fayans, Sov. J. Nucl. Phys. **48**, 995 (1988).
7. B.Friedman and V.R.Pandharipande, Nucl. Phys. **A361**, 502 (1981).
8. R.B.Wiringa, V.Fiks, and A.Fabrocini, Phys. Rev. **38**, 1010 (1988).
9. M.Kutschera, Phys. Lett. **B340**, 1 (1994).
10. V.A.Khodel and E.E.Saperstein, Phys. Reports. **92**, 183 (1982).
11. V.R.Shaginyan, Sov. J. Nucl. Phys. **40**, 728 (1984).
12. A.Bulgac and V.R.Shaginyan, Nucl. Phys. **A601**, 103 (1996).
13. P.Ring, Prog. Part. Nucl. Phys. **37**, 193 (1996).
14. S.A.Fayans and D.Zawischa, Phys. Lett. **B383**, 19 (1996).
15. G.Audi and A.H.Wapstra, Nucl. Phys. **A565**, 1 (1993).